Proceedings **206**, R. S. Averback, J. Bernholc, D. L. Nelson, Eds. (Materials Research Society, Pittsburgh, 1991), p. 691.
2. P. A. Heiney *et al.*, *Phys. Rev. Letters* **66**, 2911 (1991); J. E. Fischer *et al.*, *Science* **252**, 1288 (1991).
3. P. W. Stephens *et al.*, *Nature* **351**, 632 (1991).
4. R. M. Fleming *et al.*, *ibid.*, in press.
5. J. P. McCauley, Jr., *et al.*, *J. Am. Chem. Soc.*, in press.
6. K. Holczer *et al.*, *Synthetic Metals*, in press; P. W. Stephens *et al.*, in preparation.
7. R. M. Fleming *et al.*, *Nature* **352**, 701 (1991).
8. O. Zhou *et al.*, *ibid.* **351**, 462 (1991).
9. S. A. Safran, in *Solid State Physics*, H. Ehrenreich, F. Seitz, D. Turnbull, Eds. (Academic Press, New York, 1987), vol. 40, p. 183.
10. J. Ma, H.-Y. Choi, E. J. Mele, J. E. Fischer, *Synthetic Metals* **27**, A75 (1988).
11. D. M. Poirier *et al.*, *Science* **253**, 646 (1991).
12. C. T. Chen *et al.*, *Nature* **352**, 603 (1991).
13. J. E. Fischer, in *Chemical Physics of Intercalation*, A. P. Legrand and S. Flandrois, Eds. (Plenum, New York, 1987), p. 59.
14. R. C. Haddon *et al.*, *Nature* **350**, 320 (1991).
15. R. Tycko *et al.*, *Science* **253**, 884 (1991).
16. D. Djurado *et al.*, *Synthetic Metals* **34**, 683 (1989); P. A. Heiney *et al.*, *Phys. Rev.* **B42**, 2507 (1991).
17. S. C. Erwin and W. E. Pickett, *Science*, in press; private communication.
18. S. E. Millman and G. Kirczenow, *Phys. Rev.* **B26**, 2310 (1982).
19. D. E. Luzzi *et al.*, *J. Mat. Res.*, in press.
20. W. Andreoni, F. Gygi, M. Parrinello, in preparation.

21. We acknowledge helpful discussions with A. Cheng, P. A. Heiney, and E. J. Mele, and thank C. L. Lin for performing the magnetization measurements. This work was supported by the National Science Foundation Materials Research Laboratory Program, DMR88-19885, by NSF DMR89-01219, and by the Department of Energy, DE-FC02-86ER45254 and DE-FG05-90ER75596.

5 September 1991; accepted 20 September 1991

Clathrate Hydrate Formation in Amorphous Cometary Ice Analogs in Vacuo

DAVID BLAKE,* LOUIS ALLAMANDOLA, SCOTT SANDFORD,
DOUG HUDGINS, FRIEDEMANN FREUND

The presence of clathrate hydrates in cometary ice has been suggested to account for anomalous gas release at large radial distances from the sun as well as the retention of volatiles in comets to elevated temperatures. However, how clathrate hydrates can form in low-pressure environments, such as in cold interstellar molecular clouds, in the outer reaches of the early solar nebula, or in cometary ices, has been poorly understood. Experiments performed with the use of a modified electron microscope demonstrate that during the warming of vapor-deposited amorphous ices in vacuo, clathrate hydrates can form by rearrangements in the solid state. Phase separations and microporous textures that are the result of these rearrangements may account for a variety of anomalous cometary phenomena.

IN COLD INTERSTELLAR MOLECULAR clouds, gaseous species such as H_2O, CO, CO_2, CH_3OH, H_2CO, and NH_3 are believed to condense onto submicron silicate and carbonaceous grains to form icy mantles (*1, 2*). By a combination of processes that include gas-grain chemical reactions, ultraviolet photolysis, and cosmic-ray bombardment, these components can react further to produce small amounts of complex organic compounds (*3–7*). Icy planetesimals that probably formed through successive aggregation and agglomeration of such ice-coated grains may have carried significant amounts of prebiotic organic materials to Earth during its early history (*8*). Comets are thought to contain primitive and pristine materials from the early solar system, perhaps even unaltered interstellar grains (*1*). A knowledge of the properties of cometary ice (composition, structure state, and so forth) may therefore provide a better understanding of the types and amounts of volatiles and biogenic elements that were delivered to the early Earth.

During the past decade, several workers have probed the chemical composition and photochemical and photophysical properties of cometary and astrophysical ice analogs and compared the results with astronomical infrared data (*1, 9, 10*). In other work, the gas release properties of precometary and cometary ice analogs have been studied in order to understand the dynamics of comets and other icy solar system bodies (*11–13*). Although there have been some recent reports on structural investigations of mixed molecular ices (*14*), the crystallographic, microtextural, and phase evolution of astrophysical ice analogs specifically under high-vacuum conditions have not been investigated and are poorly understood. In order to make such observations, we modified an Hitachi H-500H Analytical Electron Microscope to enable us to study ices between 12 and 373 K (±2 K accuracy, measured at the sample) in a vacuum of 10^{-6} to 10^{-7} torr (*15*). Gas mixtures were bled into the vacuum and condensed onto cold (85 K), thin-film carbon substrates. The mixed molecular ices thus formed were characterized by transmission electron microscopy (TEM) and selected area electron diffraction (SAED). Through the use of a low electron dose imaging system, ice samples could be viewed without apparent structural damage or heating by the electron beam. We initially chose the system H_2O-CH_3OH because CH_3OH appears to be an important constituent in some cold interstellar clouds (*2, 10*) and has recently been detected in the comae of several comets (*16*).

We produced a compact, nonporous layer of amorphous ice 100 to 200 nm in thickness by condensing an H_2O:CH_3OH (2:1) gas mixture onto the 85 K substrate at a rate of 20 to 40 nm min^{-1}. Upon heating slowly at a rate of ~1 K min^{-1}, the ice remained amorphous until about 120 K, at which point broad Debye-Scherrer rings appeared in the SAED pattern. Bright-field TEM micrographs revealed the presence of two phases that were tightly intergrown on a scale length of about 0.1 μm (Fig. 1A). In the micrograph, amorphous areas appear bright and crystalline areas appear dark because diffracted electrons from the crystalline regions do not contribute to the final image. By 130 K the number of Debye-Scherrer rings had reached seven to eight (Fig. 1B). At about 145 K one of the two tightly intergrown phases sublimed, and a microporous texture was left (Fig. 1C) that produced an SAED pattern that could be indexed as the hexagonal polymorph of H_2O ice (Fig. 1D). We interpret the bright contrast features in Fig. 1C to be voids because in thin areas of the ice, the underlying carbon support film could be clearly seen within each of the features. At about 155 K the hexagonal H_2O ice rapidly sublimed.

Another sample of amorphous H_2O:CH_3OH (2:1) ice was warmed up more rapidly (~4 K min^{-1}) from 85 to 130 K. At 130 K the same SAED pattern was obtained as after slow warm-up, but the Debye-Scherrer rings were slightly sharper. In addition, a large number of single crystal spots could be seen. With the exception of a weak- to medium-intensity ring at ~3.6 Å [probably the (111) maximum of cubic H_2O ice], the powder rings and single-crystal spots could be indexed to a type II clathrate hydrate structure (space group *Fd3m*) (*17, 18*) with an *a*-parameter of 16.3 Å (Table 1) (*19*). In two earlier studies clathrate hydrates were inferred to have

---

D. Blake, Planetary Biology Branch, Mail Stop 239-4, National Aeronautics and Space Administration, Ames Research Center, Moffett Field, CA 94035.
L. Allamandola, S. Sandford, D. Hudgins, Mail Stop 245-6, Astrophysics Branch, National Aeronautics and Space Administration, Ames Research Center, Moffett Field, CA 94035.
F. Freund, Department of Physics, San Jose State University, San Jose, CA 95192.

*To whom correspondence should be addressed.

formed from amorphous, mixed molecular ice precursors on the basis of infrared spectroscopic measurements (*20*). Clathrate hydrates are crystalline phases of water ice that enclose stoichiometric amounts of guest molecules in specific cage sites in the structure. Two structure types have been described for clathrate hydrates, type I and type II, that differ primarily in the size and number of guest molecules they can enclose (*17–19*). In our system, the guest molecule (CH_3OH) is sufficiently large to result in a type II clathrate hydrate. In both the rapidly warmed and slowly warmed H_2O:CH_3OH (2:1) ices, all (hkl) values with $h + k + l = 2n + 1$ or $h + k + l = 4n$ were observed except for (111), (220), and (311). On the basis of the extinction rules for the space group $Fd3m$, the diffractions $h + k + l = 2n + 1$ and $h + k + l = 4n$ form the set b, to which only clathrate cage sites contribute intensity (*17*). This result has an interesting implication with respect to order-disorder relations in the clathrate structure: The clathrate hydrate as formed from the amorphous mixed molecular ice appears to be ordered with respect to the CH_3OH molecules in its cages, whereas the three-dimensional framework of H_2O molecules that forms the cages retains a high degree of disorder. The long-range interaction between the CH_3OH molecules that is a prerequisite for such an ordering process may be provided by H-bonding between CH_3OH and the surrounding H_2O molecules. This H-bonding is expected to cause distortions of the cages and, hence, provides a coupling mechanism between cage sites over a relatively large distance. The less-than-perfect match between observed positions and intensities of electron diffraction lines and the data for related type II clathrate hydrate structures, based on x-ray diffraction analyses, is not uncommon in this class of compounds (*19*).

In the structure of the type II clathrate hydrate, the ideal ratio of H_2O to large guest molecules is 17:1 (*18, 19*). The 2:1 ratio that we used for our first experiments requires that when the clathrate hydrate forms, the excess CH_3OH must leave the structure, probably by segregation to crystalline grain boundaries. The intergrowth of two phases observed at ~130 K and illustrated by Fig. 1A is the result of subsolidus eutectoid separation of the amorphous mixed ice into two components: The clathrate hydrate and a grain boundary phase consisting of nearly pure CH_3OH. Because the diffraction data indicated that only one crystalline phase was present, namely the type II clathrate hydrate (plus some cubic water ice as an impurity), the CH_3OH-rich grain boundary phase must have remained amorphous. Evaporation of the CH_3OH-rich amorphous component would result in a microtexture of clathrate hydrate crystals with high porosity. To validate this idea we prepared H_2O:CH_3OH (20:1) ice, in which there is not quite enough CH_3OH to saturate the large cage sites in the type II clathrate hydrate structure. When this mixed ice was deposited at 85 K it formed a compact, amorphous, and textureless layer. When warmed to 130 K, the same powder rings appeared as before. This observation confirms that the type II clathrate hydrate structure had formed (see Table 1). However, no microtexture developed at 130 K and little microporosity was observed after warming to 145 K. This observation shows that, as expected, a CH_3OH-rich grain boundary phase did not segregate from the H_2O:CH_3OH (20:1) ice during crystallization of the type II clathrate hydrate.

In addition to the electron optical studies, we recorded the infrared absorption spectra of H_2O:CH_3OH (2:1) ices that were condensed in the amorphous state at 10 K and warmed at a rate of about 1 K min^{-1}. [See (*4*) for a description of the techniques and apparatus used.] Between 120 and 130 K, a small change was noticed in the profiles of some of the CH_3OH bands. This change suggested that a structural transformation had occurred. In a new experiment the ice was doped with a small amount of CO_2 (H_2O:CH_3OH:CO_2 = 100:50:1) to act as a sensitive local probe. At 10 K the CO_2 asymmetric stretching fundamental, ν_3, peaked near 2340 cm^{-1}, as reported for another H_2O:CH_3OH mixed ice containing CO_2 (*21*). The profile of the ν_3 band changed little upon warming until 120 K, at which point a shoulder appeared at 2346 cm^{-1} (Fig. 2). The blue shift of the ν_3 band indicates that some of the CO_2 molecules were transferred into smaller, repulsive sites. These new sites were probably associated with the type II clathrate hydrate structure.

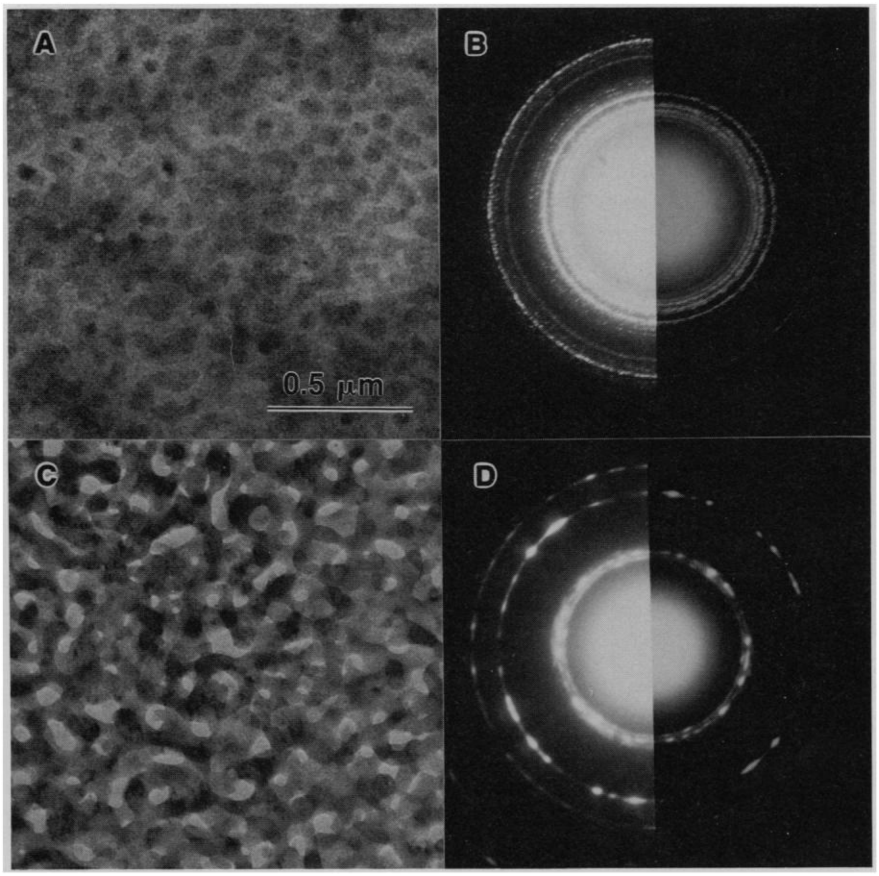

Fig. 1. TEM micrographs and SAED patterns from thermally processed 2:1 H_2O:CH_3OH ices. (**A**) Bright-field TEM micrograph of H_2O:CH_3OH (2:1) ice after subsolidus formation of the type II clathrate hydrate of methanol at a temperature (T) of 120 K. Crystallization and phase separation are apparent. (**B**) SAED pattern from a region equivalent to the ice shown in (A), T = 130 K. The powder rings can be indexed as a type II clathrate hydrate structure with an a-parameter of 16.3 Å. The right and left sides of the pattern are different exposures of the same negative. (**C**) Bright-field TEM micrograph of the H_2O:CH_3OH (2:1) ice, recorded after sublimation of the amorphous component and inversion of the clathrate hydrate to hexagonal ice (T = 150 K). Note the porous structure resulting from the original subsolidus phase separation during clathrate formation. In H_2O:CH_3OH (20:1) ice, no porosity develops after high-temperature processing. Scale is as in (A). (**D**) SAED pattern from a region equivalent to the ice shown in (C). The pattern can be indexed as the hexagonal polymorph of H_2O ice (T = 150 K).

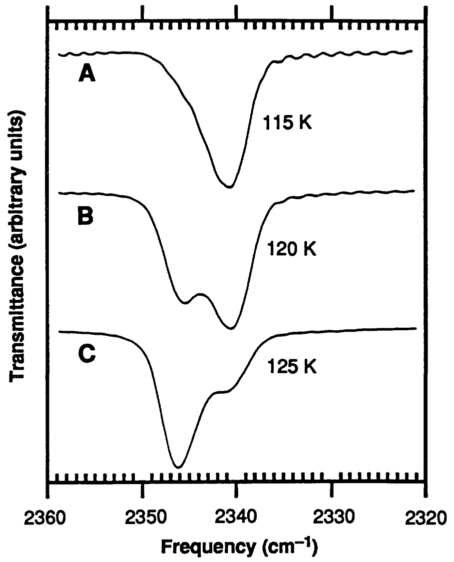

Fig. 2. Infrared spectra of the ν_3 asymmetric stretching band of CO_2 in H_2O:CH_3OH:CO_2 (100:50:1) ice deposited at 10 K and warmed at 1 K min^{-1} to temperatures of: (**A**) 115 K, (**B**) 120 K, and (**C**) 125 K. Note the appearance of a second peak near 2346 cm^{-1} in the 120 K ice. The band splitting is indicative of two distinct trapping sites within the H_2O:CH_3OH ice structure.

This assignment is supported by a recent infrared study in which a type II clathrate hydrate containing CO_2 was grown epitaxially onto a tetrahydrofuran, type II clathrate hydrate (*22*). Upon further warming to 125 K and higher, the intensity of the 2346 cm^{-1} shoulder increased relative to that of the 2340 cm^{-1} band and eventually replaced it without noticeable loss in band area. This shift of the ν_3 band of CO_2 during the transition from the amorphous mixed ice to the clathrate hydrate suggests that remote measurement of this band in astrophysical ices could yield important information about their composition, structure, and temperature history.

Early workers have proposed that the presence of clathrate hydrates in extraterrestrial ices might account for their anomalous volatile retention and release (*23*). Indeed, the subsolidus eutectoid phase separation observed during warming of amorphous, two-component H_2O:CH_3OH ices may serve to illustrate the gas release and mechanical properties of cometary ices. A well-characterized example from an entirely different class of materials is the devitrification of multicomponent glasses into glass ceramics, resulting in a tightly intergrown texture of cryptocrystalline phases and a grain boundary glass (*24*). In the case of amorphous, mixed molecular ices rich in H_2O, the subsolidus formation of a clathrate hydrate can provide a safe haven for highly volatile gases occluded in the amorphous ice during low-temperature condensation. On the other hand, in mixed molecular ices containing a large amount of volatiles and large molecules, the opposite may be true: Type II clathrate hydrates may be more dilute in the guest species than are the starting materials. A component in ~6% molar concentration is sufficient to form a type II clathrate hydrate in which all of the H_2O is in a mixed molecular ice. If the original amorphous ice is rich in large molecules, some of the occluded volatiles will be driven out of the clathrate hydrate crystals and made available for evaporation. Such evaporation would transform an initially compact layer into a highly porous layer and thereby open pathways for the escape of more gases from within. Thus, type II clathrate hydrates may play a dual role in cometary ices. On the one hand, they can act as a reservoir to keep highly volatile gases trapped in the ice at temperatures exceeding their normal sublimation point in vacuum. On the other hand, their formation from amorphous ice may drive out excess volatiles that cannot fit in the clathrate structure. Depending on the volume ratio between clathrate hydrates and the pore space, the mechanical properties of the remaining ice can be affected in various ways. In the case of ice with low porosity, the surface layer may retain much of its mechanical strength despite voluminous degassing. A highly porous architexture, however, may lead to a substantial degradation of the mechanical strength and, hence, to ejection of parts of the surface layer.

Table I. Electron diffraction results for type II clathrate CH_3OH hydrate (space group $Fd3m$); h, k, and l are crystallographic indices and a is a cubic unit cell dimension.

h, k, l	Calc.* *d*-value	Irel†	Irel‡	2:1 ice slow warm to 130 K	2:1 ice rapid warm to 130 K	20:1 ice rapid warm to 130 K
(111)	9.399	70	(w)			
(220)	5.756	8	(w)			
(311)	4.909	23	(w)			
(222)	4.697	75				
(400)	4.070	70	(w)	3.96 (w)	3.96 (s)	3.96 (m)
(331)	3.735	60	(w)	3.74 (s)		3.74 (s)
				3.61 (w)§	3.57 (m)§	3.61 (w)§
						3.52 (w)
(422)	3.323	60	(vs)	3.40 (s)	3.39 (m)	3.39 (w)
					3.27 (w)	
(333) + (511)	3.133	100	(m)	3.07 (m)	3.04 (m)	3.07 (w)
					2.98 (w)	
(440)	2.878	37	(m)		2.83 (w)	2.91 (vw)
(531)	2.752	87	(vw)	2.73 (vw)	2.74 (m)	2.73 (w)
(442)	2.713					
(620)	2.574	17				
(533)	2.483	17			2.38 (m)	
(622)	2.454					
(444)	2.350					
(551) + (711)	2.280	6		2.30 (m)	2.28 (w)	2.31 (s)
(642)	2.176				2.19 (m)	
(553) + (731)	2.119	14		2.08 (m)	2.07 (m)	2.11 (m)
(800)	2.035			1.97 (w)	1.98 (m)	1.96 (m)

*Calculated *d*-values were obtained using a = 16.3 Å [*a*-parameter for clathrate II ethanol hydrate from x-ray diffraction data (*19*)]. †Relative intensities from the type II clathrate hydrate of tetrahydrofuran (*18*). ‡Qualitative intensities from clathrate II hydrate of ethanol (*19*). §Probable (111) for cubic H_2O ice. Qualitative intensities are vs, very strong; s, strong; m, medium; w, weak; and vw, very weak.

On their highly asymmetrical paths around the sun comets are exposed to relatively short but intense warming close to perihelion. This heat will propagate into the interior, subject to the constraints of the thermal diffusivity of the ice. In view of the results for H_2O:CH_3OH ices, it is conceivable that clathrate hydrates also form deep within the cometary nucleus. If these clathrate hydrates cannot accommodate all of the volatile components formerly occluded in the amorphous ice, a grain-boundary phase will segregate (as discussed above) containing a high volatile concentration. This segregation can lead to the build-up of a sufficiently high volatile pressure to disrupt the cometary body and lead to an explosive gas discharge. Subsolidus devitrification and phase separation may be aided by latent heat released by recrystallization and by recombination of free radicals trapped in the ice. Because all the processes involve phase separation, one obvious consequence might be that the composition of the coma of a comet is not a simple function of the overall composition of the nucleus from which the gases and solid matter were expelled. The coma may be the sublimate of what could be characterized as the subsolidus eutectoid devitrification of the parent ice.

Subsolidus crystallization of compositionally complex amorphous ices may be a general and ubiquitous process. Its importance in other environments such as those present on the surfaces or in the interiors of the outer planets and icy satellites has yet to be determined.

REFERENCES AND NOTES

1. J. M. Greenberg, in *Comets*, L. L. Wilkening, Ed. (Univ. of Arizona Press, Tucson, 1982), pp. 131–163; L. J. Allamandola and S. A. Sandford, in *Dust in the Universe*, M. E. Bailey and D. A. Williams, Eds. (Cambridge Univ. Press, Cambridge, 1988), pp. 229–263.
2. A. G. G. M. Tielens, in *Interstellar Dust*, L. J. Allamandola and A. G. G. M. Tielens, Eds. (Kluwer, Dordrecht, 1989), pp. 239–262.
3. L. B. D'Hendecourt *et al.*, *Astron. Astrophys.* **158**, 119 (1986).
4. L. J. Allamandola *et al.*, *Icarus* **76**, 225 (1988).
5. M. H. Moore, B. Donn, R. Khanna, M. F. A'Hearn, *ibid.* **54**, 388 (1984).
6. R. E. Johnson, L. J. Lanzerotti, W. L. Brown, W. M. Augustiniak, C. Mussil, *Astron. Astrophys.* **123**, 343 (1983); R. E. Johnson, J. F. Cooper, L. J. Lanzerotti, G. Strazzulla, *ibid.* **187**, 889 (1987).
7. G. V. Strazzulla, V. Pirronello, G. Foti, *ibid.* **123**, 93 (1983).
8. C. F. Chyba, *Nature* **343**, 129 (1990).
9. W. Hagen *et al.*, *Chem. Phys.* **56**, 367 (1981).
10. A. G. G. M. Tielens and L. J. Allamandola, in *Physical Processes in the Interstellar Medium*, G. Morfill and M. Schaler, Eds. (Reidel, Dordrecht, 1987), pp. 333–338.
11. A. Bar-Nun *et al.*, *Phys. Rev. B* **35**, 2427 (1987).
12. S. A. Sandford and L. J. Allamandola, *Icarus* **76**, 201 (1988).
13. H. A. Kochan *et al.*, *Lunar Planet. Sci.* **XX**, 524 (1989); P. Hsuing and K. Roessler, *ibid.* **XXI**, 538 (1990).
14. A. Kouchi and T. Kuroda, *Nature* **344**, 134 (1990); A. Kouchi, *J. Cryst. Growth* **99**, 1220 (1990); A. Hallbrucker and E. Mayer, *Icarus* **90**, 176 (1991).
15. D. F. Blake *et al.*, *Proceedings of the XII International Congress of Electron Microscopy*, Seattle, WA, August 1990 (San Francisco Press, San Francisco, 1990), vol. 1, p. 594.
16. D. Bockelee-Morvan *et al.*, *Nature* **350**, 318 (1991).
17. T. C. W. Mak and R. K. McMullan, *J. Chem. Phys.* **42**, 2732 (1965).
18. J. E. Bertie and S. M. Jacobs, *ibid.* **69**, 4105 (1978).
19. P. Boutron and A. Kaufmann, *ibid.* **68**, 5032 (1978).
20. J. E. Bertie and J. P. Devlin, *ibid.* **78**, 6340 (1983); H. H. Richardson, P. J. Wooldridge, J. P. Devlin, *ibid.* **83**, 4387 (1985).
21. S. A. Sandford and L. J. Allamandola, *Astrophys. J.* **355**, 357 (1990).
22. F. Fleyfel and J. P. Devlin, *J. Phys. Chem.* **95**, 3811 (1991).
23. A. H. Delsemme and P. Swings, *Ann. Astrophys.* **15**, 1 (1952); A. H. Delsemme and D. C. Miller, *Planet. Space Sci.* **18**, 709 (1970); *ibid.*, p. 717; S. L. Miller, in *Physics and Chemistry of Ice*, E. Whalley *et al.*, Eds. (Royal Society of Canada, Ottawa, 1973), pp. 42–50; J. I. Lunine and D. J. Stevenson, *Astrophys. J. Suppl. Ser.* **58**, 493 (1985); S. Engle, J. I. Lunine, J. S. Lewis, *Icarus* **85**, 380 (1990).
24. I. Gutzow, *Contemp. Phys.* **21**, 121 (1980).
25. This work was initiated under a grant from the Director's Discretionary Fund of the National Aeronautics and Space Administration (NASA)/Ames Research Center, Moffett Field, CA. We additionally acknowledge the support of the Planetary Geochemistry Division of NASA.

13 May 1991; accepted 24 July 1991

U and Sr Isotopes in Ground Water and Calcite, Yucca Mountain, Nevada: Evidence Against Upwelling Water

J. S. STUCKLESS, Z. E. PETERMAN, D. R. MUHS

Hydrogenic calcite and opaline silica deposits in fault zones at Yucca Mountain, Nevada, have created considerable public and scientific controversy because of the possible development of a high-level nuclear waste repository at this location. Strontium and uranium isotopic compositions of hydrogenic materials were used to test whether the veins could have formed by upwelling of deep-seated waters. The vein deposits are isotopically distinct from ground water in the two aquifers that underlie Yucca Mountain, indicating that the calcite could not have precipitated from ground water. The data are consistent with a surficial origin for the hydrogenic deposits.

YUCCA MOUNTAIN, NEVADA, HAS been selected for geologic evaluation as a potential site for a high-level nuclear waste repository (*1*). Faults and fractures cutting the volcanic rocks at Yucca Mountain are commonly filled with low-temperature secondary carbonates, oxides, and silicates (hydrogenic deposits) that precipitated from aqueous solutions. Because these deposits mark the pathways of past fluid migration, an understanding of their origins is critically important in evaluating the site and predicting whether flooding of the repository is likely in the future.

In the vicinity of Yucca Mountain, trenches have been excavated across faults as part of the investigation of Quaternary tectonic activity (*2*). Trench 14, excavated across the Bow Ridge fault on the eastern side of Yucca Mountain (Fig. 1), exposes a vein-like deposit of calcium carbonate and subordinate opaline silica (Fig. 2) much wider and more complex than mineralogically similar deposits in other trenches. The origin of these veins and those at Busted Butte (Fig. 1) has been the focus of considerable controversy (*3*).

Four main origins have been proposed for the hydrogenic deposits (*4*): (i) deposition associated with pedogenic (soil-forming) processes whereby descending meteoric waters interact with surficial materials and precipitate minerals along fractures and faults; (ii) deposition from cold springs due to movement of regional or perched ground water along faults; (iii) deposition from hot water (temperature $\geqslant$ 30°C) along faults; and (iv) deposition through seismic upwelling of hot or cold water along faults as a direct result of strain release during faulting. Proponents of models that would result in flooding of the repository predict doomsday scenarios (*3*).

Early field and mineralogic studies of deposits exposed at Trench 14 and other sites suggested that the hydrogenic deposits formed by processes related to pedogenesis (*5*). Stable isotope studies showed that $\delta^{18}O$ and $\delta^{13}C$ of the vein deposits have values and relations similar to those in the local soils (*6*). Furthermore, the ground waters currently beneath Yucca Mountain would have to be greatly cooled and perhaps isotopically modified to precipitate the observed calcites (*7*).

We describe Sr and U isotopic compositions of the deposits and of possible source waters. Neither Sr nor U fractionate isotopically during precipitation of hydrogenic deposits. Isotopic identity between hydrogenic deposits and possible source waters would be permissive evidence for a genetic link, whereas isotopic disparity would preclude any direct genetic relationship (*8, 9*).

Sr is an excellent tracer in the hydrologic cycle because it is relatively abundant in water and because its isotopic composition, reported as $^{87}Sr/^{86}Sr$, can be measured with great precision and accuracy (± 0.00005 or better). Ground water attains its Sr isotopic signal at recharge and along its flow path by dissolution of or exchange with minerals in the aquifer (*8*). Differences between the isotopic composition of the ground water and that of the bulk aquifer can result from preferential dissolution of minerals with different $^{87}Sr/^{86}Sr$ values. Commonly, in rocks that are old enough to have an accumulated radiogenic Sr from the decay of ^{87}Rb, a phase with a low Rb/Sr value (for example, plagioclase) is preferentially attacked, and water is less radiogenic (lower $^{87}Sr/^{86}Sr$ value) than its host rock (*9*). However, disequilibrium between solid and liquid during mineral precipitation does not occur (*10*), and the isotopic composition of a solid and of the water from which the solid precipitated will be identical.

The Sr isotopic compositions of ground waters in the Tertiary aquifer beneath Yucca Mountain and of vein carbonates at Trench 14 and Busted Butte do not overlap significantly (Fig. 3). The 15 samples of ground water from the Tertiary aquifer have a mean $^{87}Sr/^{86}Sr$ value of 0.71092 ± 0.00074 (standard deviation), and the 28 samples of vein carbonate have a mean $^{87}Sr/^{86}Sr$ value of 0.71241 ± 0.00022 A t test shows that the mean values are significantly different ($P < 0.05$). The two water samples from the Yucca Mountain area with the largest $^{87}Sr/$

U.S. Geological Survey, Denver Federal Center, P.O. Box 25046, Denver, CO 80225.